MICROCOPY RESOLUTION TEST CHART

NATIONAL BUREAU OF STANDARDS-1963-A

AR-000-518

DEPARTMENT OF DEFENCE

DEFENCE SCIENCE AND TECHNOLOGY ORGANISATION

WEAPONS RESEARCH ESTABLISHMENT

SALISBURY, SOUTH AUSTRALIA

TECHNICAL REPORT 1779 (W)

CALCULATION OF PRESSURE DISTRIBUTIONS ON TWO
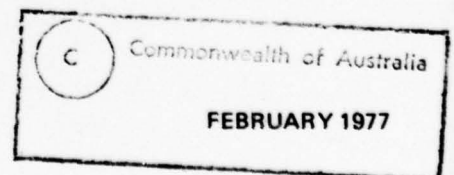AXISYMMETRIC BOATTAILED CONFIGURATIONS

M.K. HASELGROVE

DDC
OCT 6 1977
D

Approved for public release.

C Commonwealth of Australia

FEBRUARY 1977

AR-000-518

DEPARTMENT OF DEFENCE

DEFENCE SCIENCE AND TECHNOLOGY ORGANISATION

WEAPONS RESEARCH ESTABLISHMENT

14

9   WRE–TR–

TECHNICAL REPORT 1779 (W)

6

CALCULATION OF PRESSURE DISTRIBUTIONS ON TWO AXISYMMETRIC BOATTAILED CONFIGURATIONS.

10   M.K. Haselgrove

11 Feb 77

12 23p.

SUMMARY

Two published computer programs are used to calculate the pressure distributions on two axisymmetric boattailed configurations in inviscid, incompressible flow. Realistic results are obtained in the base region by extending the body surface to simulate the surface streamline separating from the base.

The results show that a favourable pressure gradient is created by replacing the rear portion of a boattail by a cylindrical section, and conversely an adverse gradient on a boattail is strengthened by the presence of a large sting on wind-tunnel models.

D D C
RECEIVED
OCT 6 1977
D

371 700

DOCUMENT CONTROL DATA SHEET

1	DOCUMENT NUMBERS	2	SECURITY CLASSIFICATION
AR Number: AR-000-518		a. Complete Document: Unclassified	
Report Number: WRE-TR-1779 (W) ✓		b. Title in Isolation: Unclassified	
Other Numbers:		c. Summary in Isolation: Unclassified	

3	TITLE
	CALCULATION OF PRESSURE DISTRIBUTIONS ON TWO AXISYMMETRIC BOATTAILED CONFIGURATIONS

4	PERSONAL AUTHOR(S):	5	DOCUMENT DATE:
	M.K. Haselgrove		February 1977

6	6.1 TOTAL NUMBER OF PAGES 22
	6.2 NUMBER OF REFERENCES: 5

7	7.1 CORPORATE AUTHOR(S):	8	REFERENCE NUMBERS
	Weapons Research Establishment ✓		a. Task: DST 76/118
			b. Sponsoring Agency:
	7.2 DOCUMENT (WING) SERIES AND NUMBER	9	COST CODE:
	Weapons Research and Development Wing TR 1779		542/AC/345

10	IMPRINT (Publishing establishment):	11	COMPUTER PROGRAM(S) (Title(s) and language(s))
	Weapons Research Establishment		

12	RELEASE LIMITATIONS (of the document):
	Approved for Public Release.

12.0	OVERSEAS	NO	P.R.	1	A		B		C		D		E	

13	ANNOUNCEMENT LIMITATIONS (of the information on these pages):

No limitation.

14	DESCRIPTORS:

a. EJC Thesaurus
   Terms

pressure distribution   axisymmetric flow
computer programs   aerodynamic configurations
inviscid flow   incompressible flow
bombs   boattail configurations
wind tunnel tests

b. Non-Thesaurus
   Terms

15	COSATI CODES:

2004
1902
0902

16	LIBRARY LOCATION CODES (for libraries listed in the distribution):

SW   SR   SD   AACA

17	SUMMARY OR ABSTRACT:

(if this is security classified, the announcement of this report will be similarly classified)

Two published computer programs are used to calculate the pressure distributions on two axisymmetric boattailed configurations in inviscid, incompressible flow.   Realistic results are obtained in the base region by extending the body surface to simulate the surface streamline separating from the base.

The results show that a favourable pressure gradient is created by replacing the rear portion of a boattail by a cylindrical section, and conversely an adverse gradient on a boattail is strengthened by the presence of a large sting on wind-tunnel models.

TABLE OF CONTENTS

LIST OF FIGURES

1. INTRODUCTION

This report describes the results of computer calculations to find the pressure distributions on two axisymmetric bomb shapes of current interest to Aerodynamic Research Group at W.R.E. The studies were initiated to augment wind-tunnel tests of the two bodies, and were particularly concerned with the effects of changes to the base geometry, including the influence of the sting on wind-tunnel models.

The calculations were limited to inviscid, axisymmetric flow solutions, and because the emphasis was on simplicity and ease of operation, the method chosen was that of Landweber(ref.1) which has recently been programmed in Fortran by Albone(ref.2). The theoretical formulation assumes incompressible flow and the results given here are for zero Mach number; however a Gothert-type correction has been included to enable approximate solutions for subsonic compressible flow to be obtained.

2. DESCRIPTION AND USE OF THE PROGRAMS

2.1 The integral equation

The method is equivalent to a representation of the body by a ring vortex distribution $\Gamma(s)$ over its surface. With the coordinate system shown in figure 1, the velocity induced at station t on the body axis by the vorticity on the surface element ds is (see, for example, reference 3):

$$U(x,t) = \frac{y_o^2(x)\,\Gamma(s)\,ds}{2\,[y_o^2(x) + (x-t)^2]^{3/2}} \; . \tag{1}$$

A consequence of representing the body surface by a vortex sheet is to replace the body interior by fluid at rest. Thus the vortex distribution must induce an interior velocity $-U_\infty$ to cancel the incident free stream. In particular, the velocity induced along the axis must be $-U_\infty$.

It can be shown that the velocity jump across a vortex sheet is minus the local vortex intensity. The condition of zero total internal velocity then gives

$$u(x) = -\Gamma(s), \tag{2}$$

where $u(x)$ is the longitudinal surface velocity at station x. Substituting (2) into (1) and integrating along the body surface gives the total velocity on the body axis, and equating to $-U_\infty$ gives the integral equation:

$$\int_O^P \frac{u(x)\,y_o^2(x)\,ds}{2\,[y_o^2(x) + (x-t)^2]^{3/2}} = U_\infty \tag{3}$$

to be satisfied at all points t between O and P. The solution of (3) gives the velocity distribution $u(x)$, and thence the pressure distribution $C_p(x)$.

A rigorous derivation of (3) and an iterative method of solution have been given in reference 1 and repeated in reference 2, which also describes Fortran programs to solve for both closed bodies and those with a parallel afterbody extending downstream to infinity. These programs need only minor alterations to be run on the W.R.E. computing system. For intending users without ready access to reference 2, listings are included in the Appendix.

The fact that the integral equation (3) for the surface velocity is satisfied on the body centreline, means that the method may not be as accurate as others which satisfy a boundary condition on the body surface, such as that of Hess and Smith(ref.4). For body shapes not too dissimilar from an ellipsoid of revolution, the solution converges to any desired degree of accuracy, but for more complicated shapes the solution may converge to a best solution and then become divergent. In such cases this best solution is usually sufficiently accurate for most practical purposes. In any case, the programs are simple to use and require only minimal computing times

compared with the more accurate methods, which determined their use in the present application. Another property of the method of solution is that corners or sudden changes of curvature in the body profile tend to be "smoothed", which is not a serious limitation since the boundary layer will have a similar effect in the real flow.

2.2   Input and output

Input to each program consists of a subroutine called BODY which can calculate the radius and surface slope of the body at any longitudinal station, and several parameters which are declared as data at the beginning of the program. For the closed-body program these are as follows:

NMAX   - the maximum number of iterations allowed (e.g., 200).

EPS   - a quantity which, when greater than the maximum difference between any two successive iterations, causes the iteration procedure to stop.

XXO   - abscissa of body nose.

XX1   - abscissa of body tail.

MACH   - Mach number, used with a Gothert-type correction to allow for compressibility effects.

For the infinite - afterbody program, the input parameters are as follows:

NMAX, EPS, MACH   - as for the closed-body program.

LENGTH - length of forebody. Note that in this program, BODY assumes the forebody to be between x = 0 and x = LENGTH, so that for complicated bodies the same basic subroutine can be used for each program.

YAFT   - radius of afterbody.

The program output consists of a listing of the Gaussian abscissae used in the numerical integration for each iteration (40 points along the body axis in the case of the closed-body program, and 30 points along the forebody axis for the infinite-afterbody program), together with the associated values of body radius and slope, non-dimensional surface velocity and pressure coefficient. The number of iterations, and maximum difference between the two final iterations, are also printed.

2.3   Body geometry

Two basic configurations of interest were studied, and designated Body-A and Body-B respectively. Two further variations of the Body-A tail geometry are referred to as A(i) and A(ii). The half-body profiles of the various configurations are given in figures 2 to 6, the x - values being in body calibres.

In those cases where the configuration has a blunt base, for example when modelling the free-flight situation, some extension of the model surface is necessary to simulate the surface streamline separating from the base. These extensions are shown on the figures as a broken line. Where a sting whose diameter is equal to the base diameter d_B is present this problem does not arise and the sting is assumed to extend downstream to infinity.

3.   RESULTS AND DISCUSSION

3.1   Standard Body-A configuration

Figure 2 shows the variation of surface pressure coefficient on the standard Body-A geometry with base flow represented by (a) a strong flow expansion behind the base; (b) a large sting of diameter d_B or alternatively, a thick parallel wake; and (c) flow separation from the base and re-attachment to a thin sting of diameter $d_B / 2$.

These examples give a wide variation in base pressure, but the influence of the base flow extends only about one base diameter upstream from the base, giving confidence in the validity of the solution ahead of this region.

If condition (c) of figure 2 is a fair representation of the base flow with a thin sting present, then condition (b) implies that a large sting can cause a significant strengthening of the adverse pressure gradient near the model base and perhaps influence the measured fin characteristics. The uncertainty regarding the best choice of base flow geometry can be partly resolved from measured base-pressure data. Such data are available from reference 5 for a variant A(i) of the Body-A configuration, which is discussed in the following section.

3.2   Configuration A(i)

The A(i) variant has the rear portion of the standard boattail, where fins are normally located, replaced by a cylindrical section which gives a 45% increase in d_B over the standard configuration, the slope of the tail cone section remaining the same at $7^o \, 40'$. The afterbody of this configuration and the calculated pressure distribution are shown in figure 3(a), with the flow assumed to separate from the base parallel to the cylindrical section. The computed values not shown for the forebody are identical with those given in figure 2 for the standard configuration. Figure 3(a) shows a strong, favourable pressure gradient along the tail cylinder, instead of the weak adverse gradient on the standard body (figure 2 condition (c)). This may result in improved fin lifting performance by reducing the tendency for flow separation in the lee-side fin root region.

Figure 3(b) shows the effect of removing the surface slope discontinuity on the A(i) afterbody by fitting a cubic polynominal to the conical and cylindrical sections between $x = 10$ and $x = 11$. Similar fairing will be effected by the boundary layer in the real flow, and wind-tunnel measurements (from reference 5) on the A(i) model, which are included on figure 3(b), compare favourably with the present results. A sting of diameter $d_B / 2$ was used for the measurements, and the data indicate some flow expansion behind the base. The calculated results can be made to agree more closely by including a small expansion in the base-flow model, as shown in figure 3(c).

3.3   Configuration A(ii)

The A(ii) configuration has a flared tail section instead of the cylindrical section of the A(i) variant. This is shown in figure 4 together with the strong, favourable pressure gradient resulting from this geometry. As mentioned above this is expected to be beneficial to fin performance, but to offset this there is a strong adverse gradient ahead of the flared section which is likely to cause some degree of flow separation, and higher drag resulting from the larger base area.

3.4   Body-A with variable afterbody slope

Pressure distributions were calculated on the Body-A forebody fitted with conical afterbodies of half angle 5°, 10°, 15° and 20° respectively. The results are displayed in figure 5. The adverse pressure gradient on the afterbody strengthens dramatically with increasing slope, but the afterbody slope has little effect on pressure coefficients ahead of about the mid-point of the central cylindrical section. If it were desired to find the maximum slope tolerated before separation became significant, a boundary-layer program could be used in conjunction with the present analysis.

3.5   Body-B results

The relatively small base of the Body-B configuration, shown in figure 6, would require the sting diameter for small wind-tunnel models to be as great or greater than d_B . Figure 6 compares the pressure distributions near the base when a sting of diameter d_B is present and absent. Consistent with the earlier results, the sting magnifies the unfavourable pressure gradient over the tail section where fins would normally be located. This should be considered when interpreting measurements of fin properties.

4.   CONCLUSIONS

Pressure distributions have been calculated on two bodies of revolution in incompressible, inviscid, axisymmetric flow. The programs of Albone(ref.2) give sufficiently accurate results with minimal user effort and computing time. Bodies with bluff bases such as boattails can be treated by assuming the body surface to be extended, thereby simulating the flow separation from the base. The choice of an appropriate base-flow model can be made more reliable if base-pressure measurements are available for comparison.

The results have shown that a favourable pressure gradient can be created by replacing the rear portion of a boattail with a cylindrical section, which may improve the effectiveness of fins mounted thereon. Conversely, fin lift measurements on wind-tunnel models may be adversely effected by the presence of a sting if its diameter is comparable to the model base diameter.

REFERENCES

No.	Author	Title
1	Landweber, L.	"The Axially Symmetric Potential Flow About Elongated Bodies of Revolution". Rep. David Taylor Model Basin 761, 1951.
2	Albone, C.M.	"Fortran Programmes for Axisymmetric Potential Flow Around Closed and Semi-Infinite Bodies". Aero. Res. Council, C.P. No. 1216, 1972.
3	Lamb, H.	"Hydrodynamics" New York, Dover. 1945
4	Hess, J.L. and Smith, A.M.O.	"Calculation of Potential Flow About Arbitrary Bodies". Prog. Aero. Sciences, Vol.8, 1967
5	Robinson, M.L.	"Stability Enhancement of Bomb Configurations". WRE-TR-1792 (W), 1977

APPENDIX I

PROGRAM LISTINGS

(a)   Closed-body program

```
C       PROGRAM FOR CLOSED AXISYMMETRIC BODY
        DIMENSION A(40),X(42),F(42),F1(40),F(40),F1(40),F2(40),X1(40),U(42
     1   ),CP(42),XK(40,40)   ,F2(40)
C       NMAX IS MAX NO OF ITERATIONS ALLOWED. EPS IS ABSOLUTE ERROR LIMIT
C       BETWEEN ITERATIONS AT CONVERGENCE. XX0,XX1 ARE FORE AND AFT
C       ABSCISSAE OF BODY. S/R BODY GENERATES ORDINATE FB AND SLOPE F1B OF
C       BODY AT EACH ABSCISSA XB.
        REAL MACH
        DATA NMAX,EPS/ 50,0.0001/
        DATA XX0,XX1/0.0,1.0/
        DATA MACH/0.0/
        REAL*8 ADUM(20)   /.0045212771,.0104982845,.0164210584,.0222458492,
     1   .0279370070,.0334601953,.038782168,.0438709082,.0486958076,
     2   .053227847,.0574397691,.0613062425,.0648040135,.0679120458,
     3   .0706116474,.0728865824,.0747231691,.0761103619,.0770398182,
     4   .0775059490/
        REAL*8XDUM(20)    /.99823771  ,.990726239 ,.97725995,.957916819,
     1   .932812808,.902098807,.865959503,.824612231,.778305651,
     2   .727318255,.671956685,.61255389,.549467125,.483075802,.413779204
     3   ,.341994091,.268152185,.192697581,.116084071,.038772418/
        BETSQ=1-MACH*MACH
        BETA=SQRT(BETSQ)
        XMID=(XX0+XX1)/2.
        CALL BODY(XMID,YMID,F1B)
        YMID=YMID*BETA
        F1B=F1B*BETA
        DO 2 K=1,20
        KK=41-K
        A(K)=ADUM(K)
        A(KK)=A(K)
        X(KK)=XDUM(K)
     2  X(K)=-XDUM(K)
        DO 8 K=1,40
        X(K)=0.5*(X(K)*(XX1-XX0)+XX1+XX0)
        XB=X(K)
        CALL BODY(XB,FB,F1B)
        FB=FB*BETA
        F1B=F1B*BETA
        F(K)=FB
        F1(K)=F1B
        F2(K)=F1B
        X1(K)=(X(K)-XX0)*(XX1-X(K))
        F1(K)=1./SQRT(1.+F1(K)*F1(K))
     8  F(K)=F(K)*F(K)
        XK0=XK1((XX1-XX0)/(2.*YMID))
        DO 3 I=1,40
        FOFT=F(I)/X1(I)
        XL=SQRT(1./FOFT)
        XK2=(1.+XK0)/(1.+XK1(XL))
        SUM=0.
        DO 4 J=1,40
        XDIF=(X(J)-X(I))*(X(J)-X(I))
        XK(I,J)=F(J)/SQRT((XDIF+F(J))**3)
        GXT=FOFT*X1(J)
```

```
      XKDASH=GXT/SQRT((XDIF+GXT)**3)
    4 SUM=SUM+A(J)*(XK(I,J)-XKDASH)
      E(I)=1.-0.25*(1.+XK0)*(XX1-XX0)*SUM-XK2
      E1(I)=(E(I)+XK0)/(1+XK0)
    3 U(I)=(1+XK0)*F1(I)
      N=0
      EMAX=100
    5 N=N+1
      FLAST=EMAX
      DO 6 I=1,40
      U(I)=U(I)+F1(I)*E(I)
      SUM=0.
      DO 7 J=1,40
    7 SUM=SUM+A(J)*XK(I,J)*(E(J)-E(I))
    6 E2(I)=F1(I)*F(I)-.25*SUM*(XX1-XX0)
      DO 13 K=1,40
   13 F(K)=F2(K)
      EMAX=ABS(E(1))
      DO12 K=1,40
      IF(ABS(E(K)).GT.EMAX)EMAX=ABS(E(K))
   12 CONTINUE
      IF(FLAST-EMAX) 18,17,17
   17 IF(EMAX.GT.EPS.AND.N.LT.NMAX) GO TO 5
   18 WRITE(6,14)N,EMAX     ,MACH
   14 FORMAT(20H NO. OF ITERATIONS =,I3,10X,13H MAX. ERROR =,F15.7,
     1   10X,9HMACH NO.=,F5.3//)
      DO 9 K=1,40
      F(K)=SQRT(F(K))
      F(K)=F(K)/BETA
      F2(K)=F2(K)/BETA
      U(K)=1+(U(K)-1)/BETSQ
      IF(MACH-0.1) 29,29,19
   29 CINC=1-U(K)*U(K)
      CP(K)=CINC+0.25*MACH*MACH*CINC*CINC
      GO TO 9
   19 CP(K)=((1-0.2*MACH*MACH*(U(K)*U(K)-1))**3.5-1)/(0.7*MACH*MACH)
    9 CONTINUE
      WRITE(6,15)
   15 FORMAT(6X,2H X,13X,2H Y,12X,6H DY/DX,7X,9H VELOCITY,3X,15H PRESS.
     1COEFFT.   )
      WRITE(6,16)(X(K),F(K),F2(K),U(K),CP(K),K=1,40)
   16 FORMAT(3(F10.6,6X),F8.4,6X,F8.4)
C
   37 STOP
      END

      FUNCTION XK1(B)
      IF(B-1.0001)3,3,1
    3 IF(B-0.9999)2,4,4
    4 XK1=0.5
      RETURN
    1 C=B*B
      D=SQRT(C-1.)
      E=ALOG(B+D)*B
      XK1=(F-D)/(C*D-E)
      RETURN
    2 C=B*B
      D=SQRT(1.-C)
      F=ALOG((1.+D)/B)*C
      XK1=(D-F)/(2.*D*D*D-D+E)
      RETURN
      END
```

(b)   Infinite - afterbody program

```
C      PROGRAM FOR BODY EXTENDING TO INFINITY
       DIMENSION A(60),X(60),F1(60),F(60),E1(60),E2(60),U(60),F(60),CP(60
      1 ),F2(60),XK(60,60)
C   NMAX IS MAX NO OF ITERATIONS ALLOWED. CONVERGENCE WHEN MAX DIFFERENCE
C   BETWEEN ITERATIONS IS L.E. EPS. XX0 IS ABSCISSA OF NOSE(N.B. JUNCTION
C   OF BODY/AFTERBODY IS AT X=0). YAFT IS RADIUS OF PARALLEL AFTERBODY.
C   S-R BODY GENERATES RADIUS FB AND SLOPE F1B AT EACH ABSCISSA XB
       REAL LENGTH
       REAL MACH
       DATA NMAX,EPS/ 50,0.0001/
       DATA LENGTH,YAFT /2.268,0.5/
       DATA MACH/0.0/
       REAL*8 ADUM(15)   /.0079681925,.0184664683,.0287847079,.0387991926,
      1 .0484026728,.0574931562,.0659742299,.0737559747,.0807558952,
      2 .0868997872,.0921225222,.0963687372,.0995934206,.101762390,
      3 .102852653/
       REAL*8 XDUM(15)   /.996893484,.983668123,.960021865,.926200047,
      1 .862560536,.829565762,.767777432,.697850495,.620526183,.536624148
      2 ,.447033377,.352704726,.254636926,.153869914,.0514718426/
       BETSQ=1-MACH*MACH
       BETA=SQRT(BETSQ)
       YAFT=YAFT*BETA/LENGTH
       XX0=-1.
       DO 2 K=1,15
       KK=31-K
       A(K)=ADUM(K)
       A(KK)=A(K)
       X(K)=XDUM(K)
       X(KK)=X(K)
     2 X(K)=-X(K)
       DO 17 K=1,30
       KK=30+K
       A(KK)=A(K)
    17 X(KK)=X(K)
       DO 8 K=1,30
       X(K)=0.5*XX0*(1.-X(K))
       XB= LENGTH*(X(K)+1.)
       CALL BODY(XB,FB,F1B)
       FB=FB/ LENGTH
       FB=FB*BETA
       F1B=F1B*BETA
       F(K)=FB*FB
       F1(K)=1./ SQRT(1.+F1B*F1B)
       F2(K)=F1B
     8 A(K)=0.25*XX0*A(K)
       DO14K=31,60
       X(K)=(1.+X(K))/(1.-X(K))
       F(K)=YAFT*YAFT
       F1(K)=1.
       F2(K)=0.
    14 A(K)=-0.25*(1.+X(K))*(1.+X(K))*A(K)
       DO 3 I=1,60
       FOFT=F(I)/(X(I)-XX0)
       E(I)=0.
```

```
      DO 4 J=1,60
      XDIF=(X(J)-X(I))*(X(J)-X(I))
      XK(I,J)=F(J) / SORT((XDIF+F(J))**3)
      GXT=FDFT*(X(J)-XX0)
      XKDASH=GXT/(XDIF+GXT)**1.5
    4 E(I)=E(I)+A(J)*(XK(I,J)-XKDASH)
      E1(I)=E(I)
    3 U(I)=F1(I)
      N=0
    5 N=N+1
      EMAX=0
      DO6 I=1,60
      U(I)=U(I)+F1(I)*E(I)
      F2(I)=F1(I)*E(I)
      DO 7 J=1,60
    7 F2(I)=F2(I)+A(J)*XK(I,J)*(E(J)-E(I))
    6 CONTINUE
      DO 12 I=1,60
      E(I)=F2(I)
   12 IF( ABS(E(I)).GT.EMAX) EMAX= ABS(E(I))
      IF(EMAX.GT.EPS.AND.N.LT.NMAX)GO TO 5
      WRITE(6,10)N,EMAX  ,MACH
   10 FORMAT(20H NO. OF ITERATIONS =,I3,10X,13H MAX. ERROR =,F15.7,
     1   10X, 10HMACH NO.=    ,F4.2,//)
   34 DO 9 K=1,60
      E(K)= SORT(E(K))
      E(K)=LENGTH*E(K)/BETA
      X(K)=LENGTH*(X(K)+1.)
      F2(K)=F2(K)/BETA
      U(K)=1+(U(K)-1)/BETSO
      IF(MACH-0.1) 29,29,19
   29 CINC=1-U(K)*U(K)
      CP(K)=CINC+0.25*MACH*MACH*CINC*CINC
      GO TO 9
   19 CP(K)=((1-0.2*MACH*MACH*(U(K)*U(K)-1))**3.5-1)/(0.7*MACH*MACH)
    9 CONTINUE
      WRITE(6,15)
   15 FORMAT(6X,2H X,13X,2H Y,12X,6H DY/DX,7X,9H VELOCITY,3X,
     1 14H PRESS. COEFT.)
      WRITE(6,16)(X(K),E(K),F2(K),U(K),CP(K),K=1,40)
   16 FORMAT(F10.5,6X,F10.6,6X,F10.6,6X,F8.4,6X,F8.4)
    C
   42 STOP
      END
```
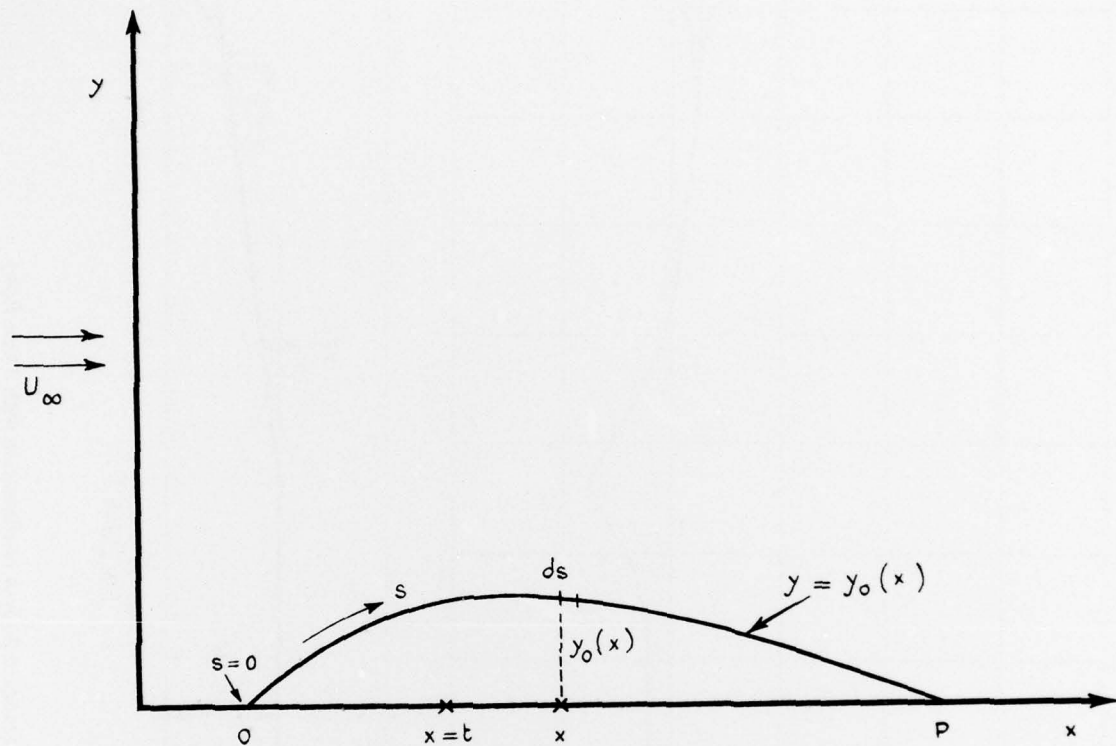
Figure 1. Coordinate system
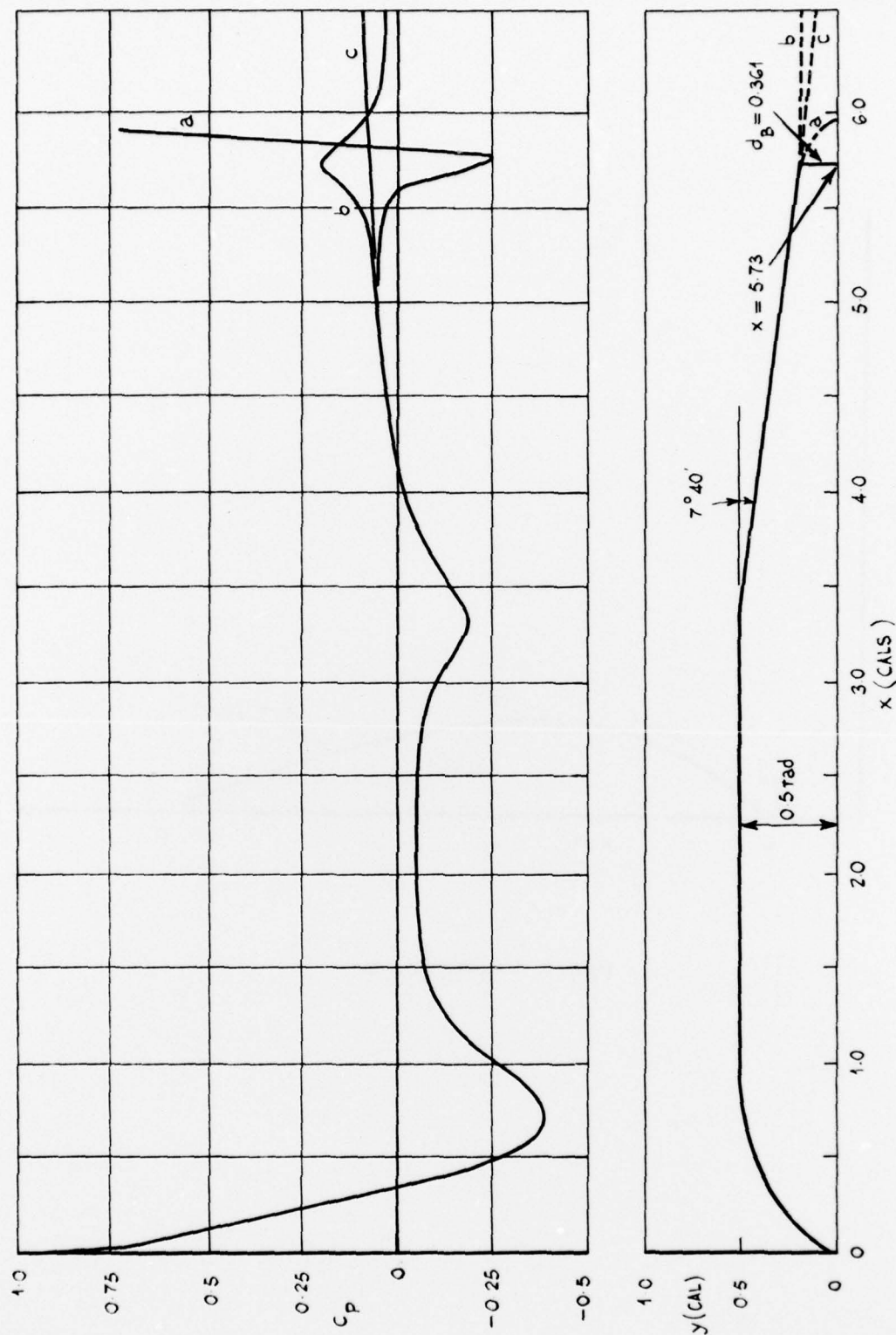
Figure 2. Standard Body-A configuration with 3 base flows
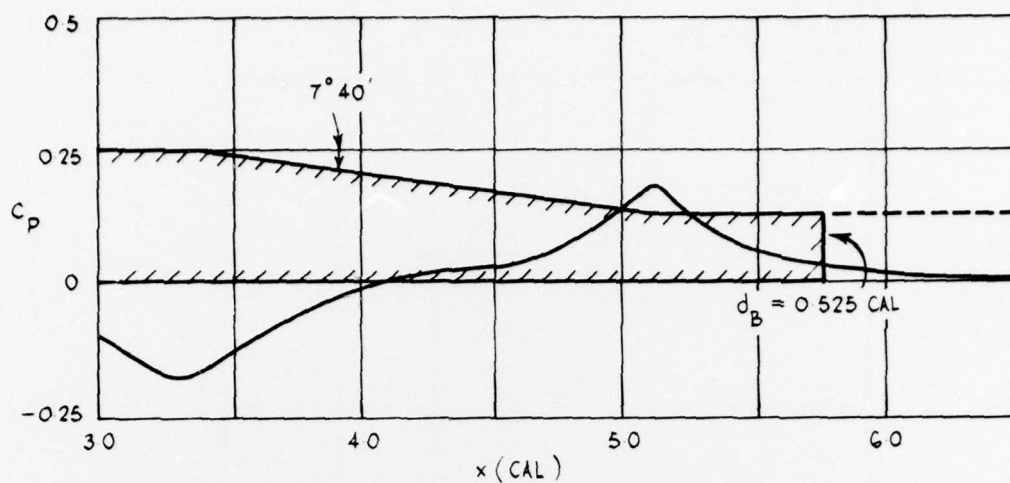
(a) Basic cone-cylinder
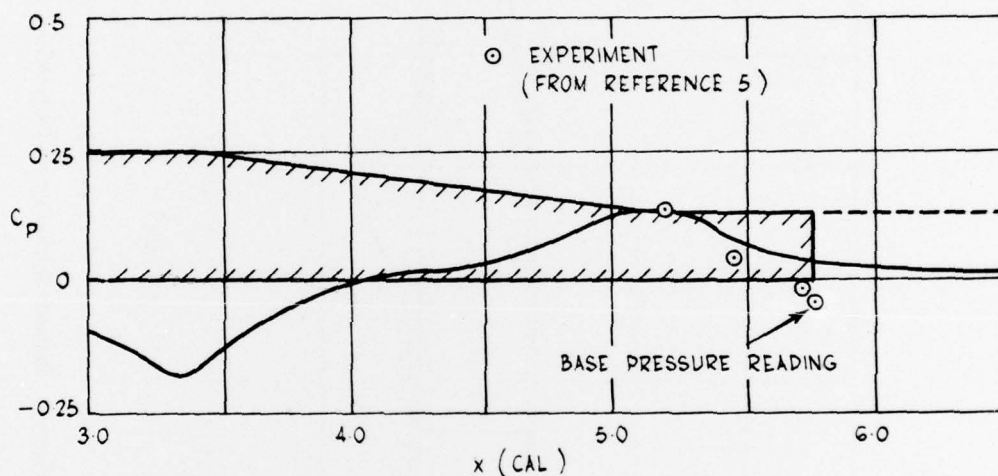
(b) With fairing
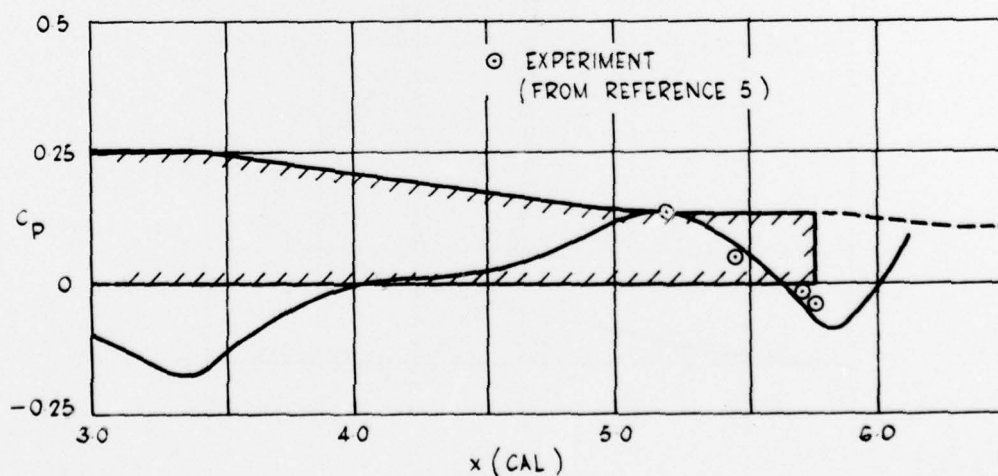
(c) Modified base flow

Figure 3. Pressure distributions on A(i) afterbody
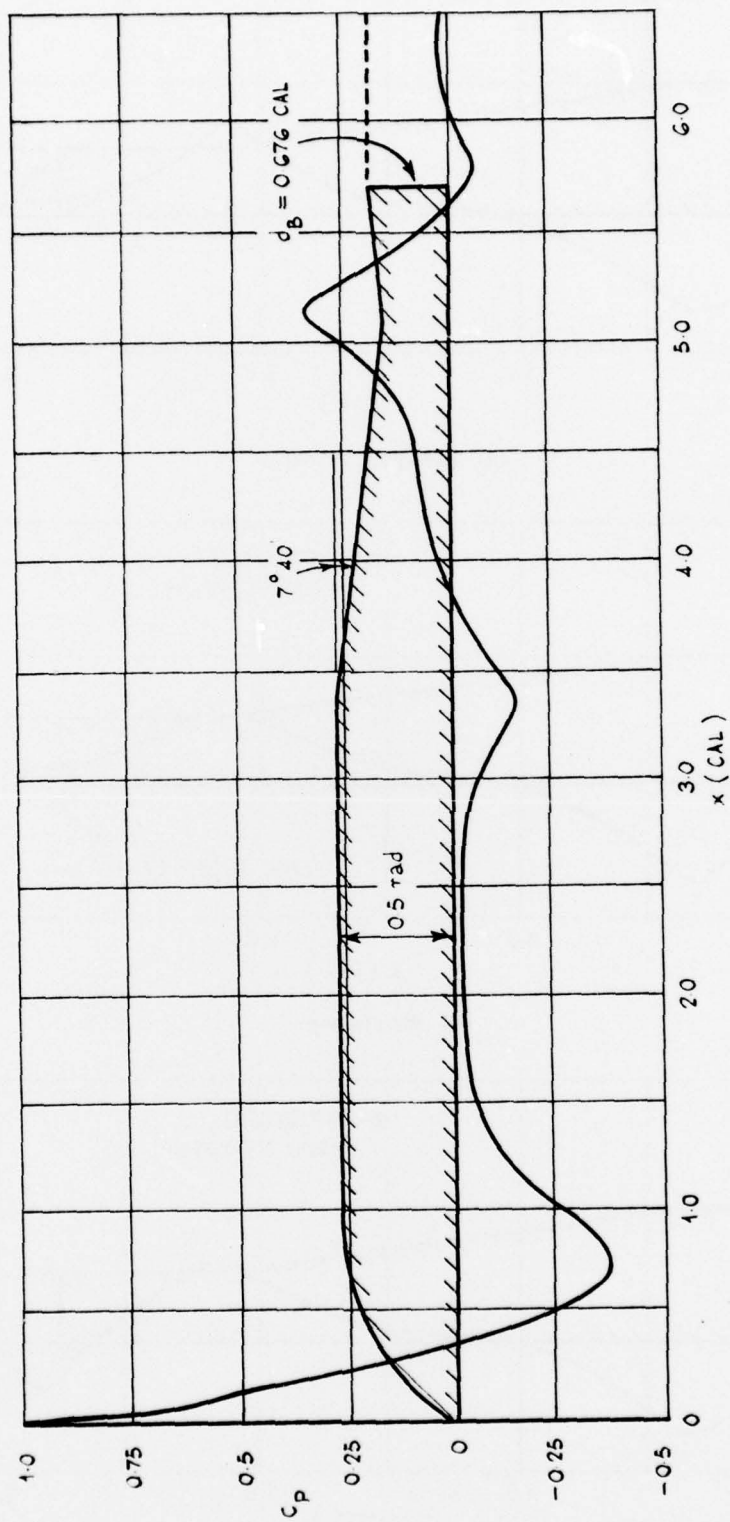
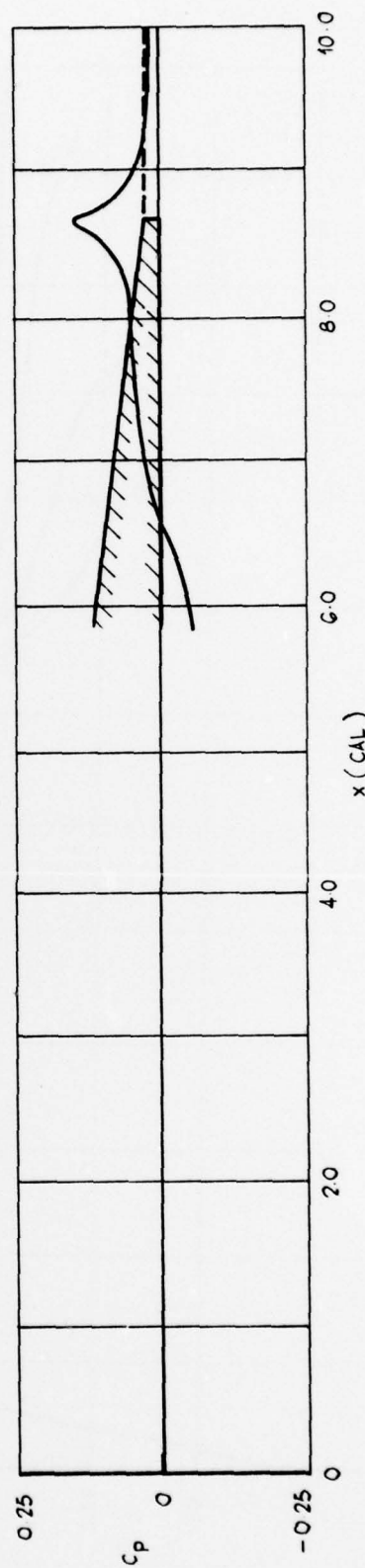Figure 4. Pressure distribution on Body-A(ii)
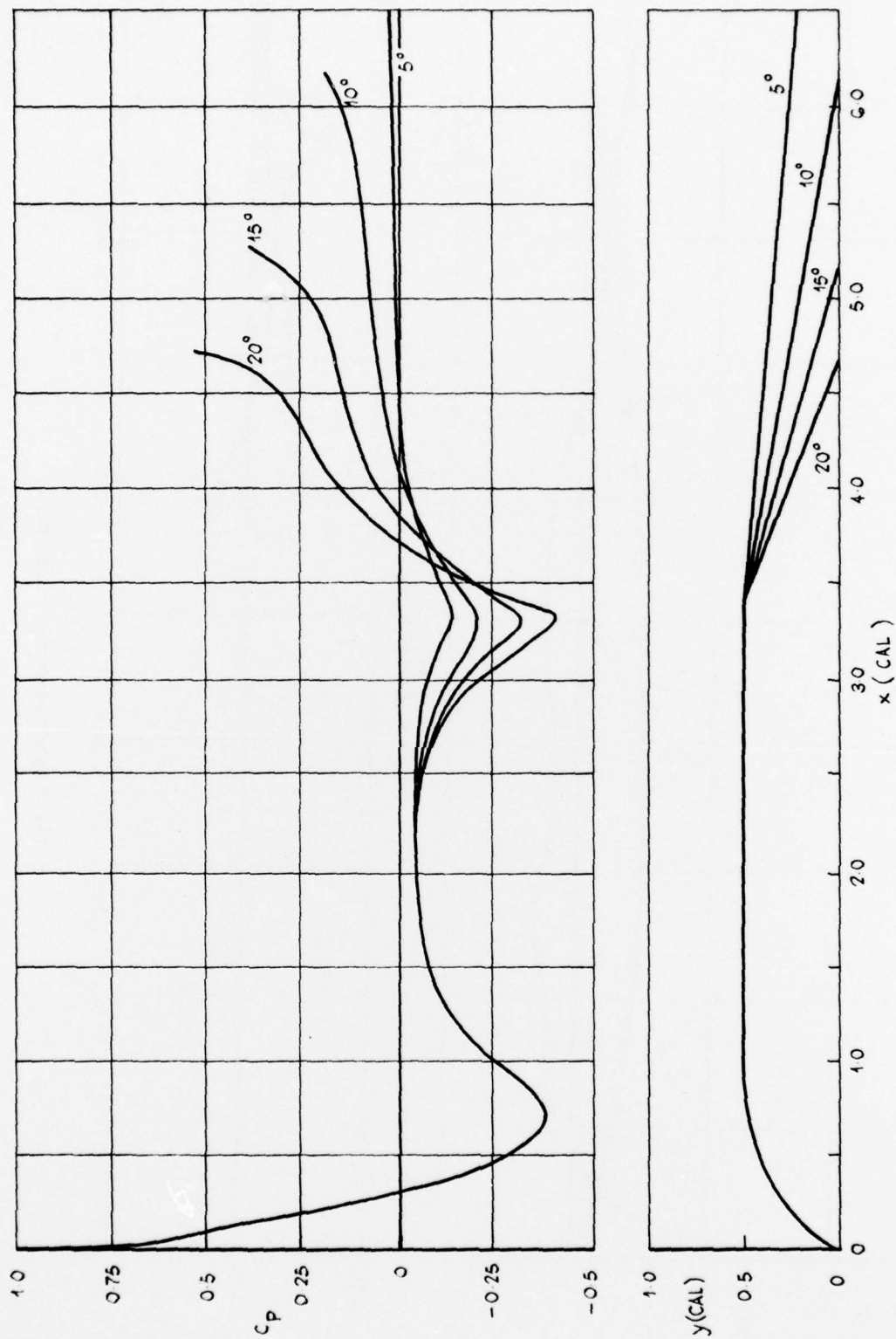
Figure 5. Body-A with variable afterbody slope
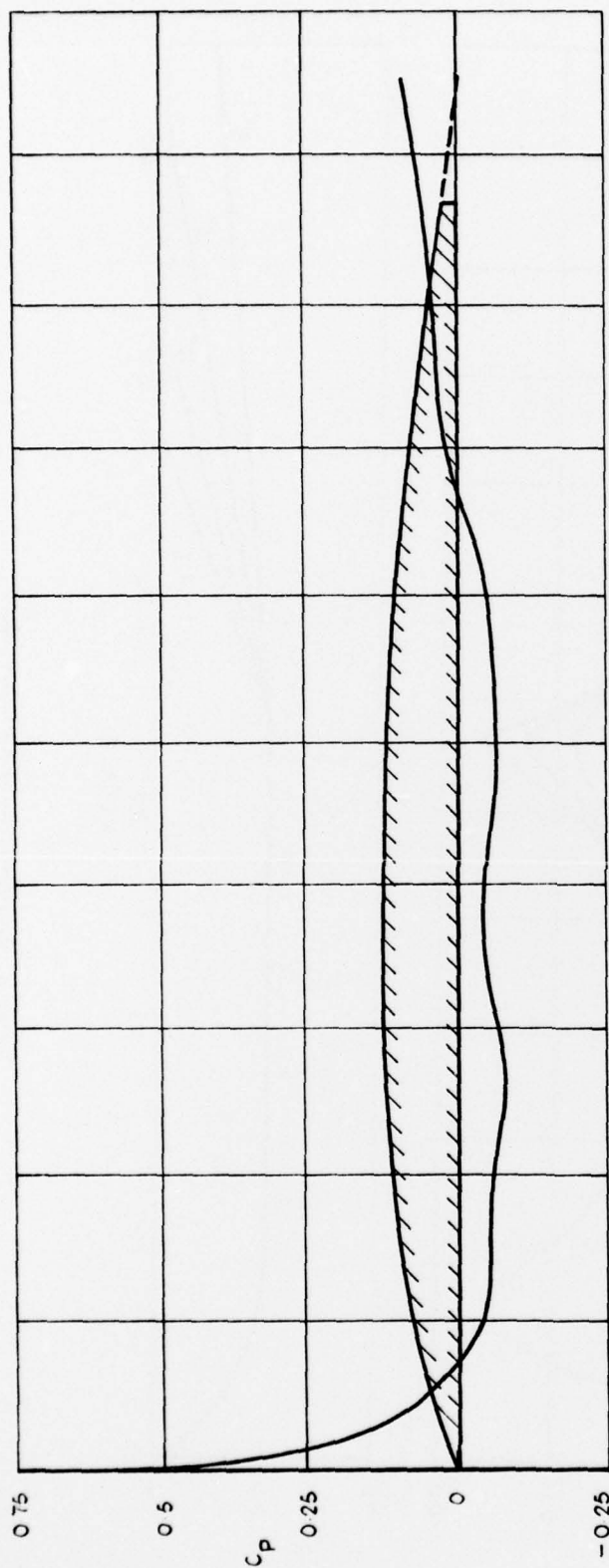
(a) Free separation at base

(b) Sting of diameter d_B = 0.201 cal

Figure 6. Pressure distributions on Body-B

DISTRIBUTION

Copy No.

In India

Aeronautical Development Establishment, Bangalore	31
Indian Institute of Science, Bangalore (Department of Aero. Engineering)	
(Attention: Professor R. Narasimha)	32
National Aeronautical Lab., Bangalore	33

In Canada

D.R.E.V., Valcartier	
(Attention: Mr. M. Laviolette)	34
N.A.E., *Ottawa*	
(Attention: Mr. L. Ohman)	35
T.T.C.P., Canadian National Leader, Panel W-2	36 - 39

In United States

Counsellor, Defence Science, Washington	40 - 41
Defence Research and Development Attache, Washington	42
T.T.C.P., U.S. National Leader, Panel W-2	43 - 46
Air Force Armament Testing Laboratory	
(Attention: Mr. C. Butler)	47
Arnold Engineering Development Center, Library	48
Ballistic Research Laboratory, Library	
(Attention: Dr. C.A. Murphy)	49
Edgewood Arsenal, Library	50
N.A.S.A.	
Ames Research Centre, Library	51
Langley Research Center, Library	52
Lewis Research Centre, Library	53
Marshall Space Flight Center, Library	54
Picatinny Arsenal	
(Attention: Mr. A. Lock)	55
Redstone Arsenal	
(Attention: Mr. R. Deep)	56
Naval Surface Weapons Center	
White Oak	
(Attention: Mr. S. Hastings)	57
Dahlgren, Library	58
Naval Ship Research and Development Center, Library	59
Naval Weapons Center	
(Attention: Dr. A. Maddox)	60

Copy No.

Copy No.

University of Melbourne

    (Attention: Professor P. Joubert)   103

University of N.S.W.

    (Attention: Professor P. Fink)   104

University of Sydney, Department of Aero. Engineering

    (Attention: Professor G. Bird)   105

University of Tasmania

    (Attention: Professor A. Oliver)   106

INTERNAL

Director, Weapons Research Establishment	107
Chief Superintendent, Weapons Research and Development Wing	108
Superintendent, Aerosopace Division	109
Head, Ballistic Composite	110
Principal Officer, Aerodynamic Research Group	111
Principal Officer, Dynamics Group	112
Principal Officer, Flight Research Group	113
Principal Officer, Ballistic Studies Group	114
Author	115
W.R.E. Library	116 - 117
Spare Copies	118 - 137
A.D. Library	138 - 139